Laser-field-induced surface-hopping method for the simulation and control of ultrafast photodynamics

Roland Mitrić,[1] Jens Petersen,[2] and Vlasta Bonačić-Koutecký[2]
[1]*Department of Physics, Freie Universität Berlin, Arnimallee 14, 14195 Berlin, Germany*
[2]*Department of Chemistry, Humboldt-Universität zu Berlin, Brook-Taylor-Str. 2, 12489 Berlin, Germany*
(Received 13 August 2008; published 15 May 2009)

We present the semiclassical laser-field-induced surface-hopping method for the simulation and control of coupled electron-nuclear dynamics in complex molecular systems including all degrees of freedom. Our approach is based on the Wigner representation of quantum mechanics. The combination of the molecular dynamics "on the fly" employing quantum initial conditions with the surface-hopping procedure allows for the treatment of the electronic transitions induced by the laser field. Our semiclassical approach reproduced accurately exact quantum dynamics in a two-electronic-state model system. We demonstrate the scope of our method on the example of the optimal pump-dump control of the trans-cis isomerization of a prototypical Schiff base molecular switch. Our results show that selective photochemistry can be achieved by shaped laser pulses which open new dynamical pathways by suppressing the isomerization through the conical intersections between electronic states.

DOI: 10.1103/PhysRevA.79.053416 PACS number(s): 32.80.Qk, 31.15.xg, 82.37.Vb, 82.50.Pt

I. INTRODUCTION

The simulation and control of ultrafast laser-driven dynamics in complex molecular systems is a challenge due to a daunting effort needed to solve the time-dependent Schrödinger equation. In particular, the ultrafast photochemistry involves the coupling of electron and nuclear dynamics leading to the breakdown of the Born-Oppenheimer adiabatic approximation. In this context, methods employing classical trajectories propagated in the framework of the molecular dynamics (MD) "on the fly" using *ab initio* or semiempirical quantum-mechanical methods for the electronic structure represent a viable semiclassical approach [1]. The Wigner representation of quantum mechanics [2,3] is particularly suitable for the development of semiclassical methods for simulation and control of ultrafast processes since it has a well-defined classical limit. Moreover, nuclear quantum effects such as, for example, tunneling [4] can be systematically included.

The control of molecular processes by shaped laser fields [5–7] opens a perspective for applications in which the light is used as photonic catalyst in chemical reactions. Following the theoretical proposal of the "closed loop learning" (CLL) scheme by Judson and Rabitz [8] numerous experiments have been realized, in which processes such as molecular fragmentation [9,10], isomerization [11], or ionization [12] are controlled. The idea of the CLL approach is to use a laser system with a pulse shaper to produce pulses which in the interaction with the quantum system initiate desired photochemical or photophysical processes. The shape of these pulses is optimized using an evolutionary algorithm maximizing the yield of the desired product or process. The theoretical counterpart of this procedure is the optimal control theory [13,14], which has provided fundamental understanding of the mechanisms responsible for the control of molecular fragmentation [10], ionization [12], and isotope selection [15,16]. However, these achievements have so far been limited to low dimensional systems in which the explicit numerical solution of the time-dependent Schrödinger equation is feasible.

Recently, the Wigner distribution approach has been developed and successfully applied to the simulation of time-resolved pump-probe spectra [1] as well as to the control of ground-state [17] and excited-state [18] dynamics. However, due to the fact that the interaction with the laser field has been described using perturbation theory, the method is limited only to processes in relatively weak fields. Therefore, the development of new theoretical methods for the simulation of laser-driven dynamics using moderately strong laser fields (below the multielectron ionization limit) is particularly desirable. Such fields open a very rich manifold of pathways for the control of ultrafast dynamics, e.g., by exploiting quantum effects such as Rabi oscillations between electronic states.

In this paper, we present a semiclassical approach for the simulation and control of the laser-driven coupled electron-nuclear dynamics in complex molecular systems including all degrees of freedom. This stochastic "field induced surface-hopping" (FISH) method is based on the combination of quantum electronic state population dynamics with classical nuclear dynamics carried out "on the fly" without precalculation of potential-energy surfaces. The idea of the method is to propagate independent trajectories in the manifold of adiabatic electronic states and allow them to switch between the states under the influence of the laser field. The switching probabilities are calculated fully quantum mechanically. Thus, the purpose of this paper is the presentation of a generally applicable method for the treatment of the laser-driven photodynamics and the illustration of its scope.

II. METHOD

The laser-driven multistate dynamics can be described using the semiclassical limit of the quantum Liouville–von Neumann (LvN) equation $i\hbar\dot{\hat{\rho}}=[\hat{H}_0-\vec{\mu}\cdot\vec{E}(t),\hat{\rho}]$ for the den-

sity operator $\hat{\rho}$. $\hat{H}_0$ represents the field-free electronic Hamiltonian for a molecular system with several electronic states in the Born-Oppenheimer approximation and the interaction with the laser field $\vec{E}(t)$ is described using the dipole approximation. In the Wigner representation, for a system with two electronic states (e and g), the commutators in the quantum LvN equation reduce in the lowest semiclassical limit to the classical Poisson brackets [3]. The equations for the phase-space representation in coordinates $\mathbf{q}$ and momenta $\mathbf{p}$ of the density-matrix elements $\rho_{gg}(\mathbf{q},\mathbf{p},t)$, $\rho_{ge}(\mathbf{q},\mathbf{p},t)$, and $\rho_{ee}(\mathbf{q},\mathbf{p},t)$ read as

$$\dot{\rho}_{gg} = \{H_g, \rho_{gg}\} - \frac{2}{\hbar}\mathrm{Im}[\vec{\mu}_{ge} \cdot \vec{E}(t)\rho_{eg}], \tag{1}$$

$$\dot{\rho}_{ge} = -i\omega_{ge}\rho_{ge} + \frac{i}{\hbar}\vec{\mu}_{ge} \cdot \vec{E}(t)(\rho_{ee} - \rho_{gg}), \tag{2}$$

$$\dot{\rho}_{ee} = \{H_e, \rho_{ee}\} - \frac{2}{\hbar}\mathrm{Im}[\vec{\mu}_{eg} \cdot \vec{E}(t)\rho_{ge}], \tag{3}$$

where curly braces denote the Poisson brackets, H_g and H_e are the Hamiltonian functions for the ground and excited states. The quantity ω_{ge} is the energy gap between the ground and excited states, $\vec{\mu}_{eg}$ and $\vec{\mu}_{ge}$ denote the transition dipole moments, and $\vec{E}(t)$ is the electric field. In order to calculate the population transfer between the ground and excited electronic states induced by the laser field $\vec{E}(t)$, which is reflected in the change in ρ_{ee} and ρ_{gg}, the coherence ρ_{ge} is needed. It can be obtained in analytic form by integrating Eq. (2):

$$\rho_{ge}(t) = \frac{i}{\hbar}\exp(i\omega_{eg}t)\int_0^t d\tau \exp(i\omega_{eg}\tau) \times \vec{\mu}_{ge} \cdot \vec{E}(\tau)[\rho_{ee}(\tau) - \rho_{gg}(\tau)]. \tag{4}$$

By inserting this expression in Eq. (3) the rate of the change of the diagonal density-matrix element $\dot{\rho}_{ee}$ which determines the population of the excited electronic state becomes

$$\dot{\rho}_{ee} = \{H_e, \rho_{ee}\} - \frac{2}{\hbar^2}\mathrm{Re}\left\{\vec{\mu}_{eg} \cdot \vec{E}(t)\exp(i\omega_{eg}t) \times \int_0^t d\tau \exp(i\omega_{eg}\tau)\vec{\mu}_{ge} \cdot \vec{E}(\tau)[\rho_{ee}(\tau) - \rho_{gg}(\tau)]\right\}. \tag{5}$$

The time evolution of the phase-space function $\rho_{ee}(\mathbf{q},\mathbf{p},t)$ can be separated into two physical contributions. The term $\{H_e,\rho_{ee}\}$ corresponds to the phase-space density flow within the excited electronic state e, while the second term in Eq. (5) describes the population transfer between the electronic states. In our FISH approach we represent the phase-space functions $\rho_{ee}(\mathbf{q},\mathbf{p},t)$ and $\rho_{gg}(\mathbf{q},\mathbf{p},t)$ by independent trajectories propagated in the ground and excited electronic states, respectively. Thus, if the finite number of trajectories N_{traj} is employed, $\rho_{ee}(\mathbf{q},\mathbf{p},t)$ can be represented by a swarm of time-dependent δ functions $\rho_{ee}(\mathbf{q},\mathbf{p},t) = \frac{1}{N_{traj}}\sum_i \delta(\mathbf{q}-\mathbf{q}_i^e(t;\mathbf{q}_0,\mathbf{p}_0))\delta(\mathbf{p}-\mathbf{p}_i^e(t;\mathbf{q}_0,\mathbf{p}_0))$, where $(\mathbf{q}_i^e,\mathbf{p}_i^e)$ represents a trajectory propagated in the excited electronic state e [1]. The population transfer between the electronic states is achieved by a process in which the trajectories are allowed to hop between the states. Notice that this hopping procedure is related to Tully's surface-hopping method [20] which has been developed in order to describe field-free nonadiabatic transitions in molecular systems. However, in our case the nonadiabatic coupling between the states is induced by the laser field. The hopping probability $P_{g\to e}$ can be calculated from the rate of change of the excited-state population, normalized to the population of the ground state according to $P_{g\to e} = \frac{(\dot{\rho}_{ee} - \{H_e,\rho_{ee}\})\Delta t}{\rho_{gg}}$. Hence, the probability that a trajectory which resides in the electronic state g at the time step t switches to the electronic state e within the time step Δt is given by

$$P_{g\to e}(t+\Delta t) = -\frac{2\Delta t}{\hbar^2\rho_{gg}}\mathrm{Re}\left\{\vec{\mu}_{eg} \cdot \vec{E}(t)\exp(i\omega_{eg}t)\int_0^t d\tau \times \exp(i\omega_{eg}\tau)\vec{\mu}_{ge} \cdot \vec{E}(\tau)[\rho_{ee}(\tau) - \rho_{gg}(\tau)]\right\}. \tag{6}$$

The simulation of the laser-induced dynamics is performed in the following three steps: (i) we generate an ensemble of trajectories by sampling, e.g., the canonical Wigner distribution function in the ground state. (ii) For each trajectory which is propagated in the framework of MD "on the fly", we calculate the density-matrix elements ρ_{ee}, ρ_{gg}, and ρ_{ge} by numerical integration. If the initial state is a pure state and dissipative effects can be neglected, as it is in our case, the set of Eqs. (1)–(3) is equivalent to the time-dependent Schrödinger equation in the representation of adiabatic electronic states:

$$i\hbar\dot{c}_i(t) = E_i(\mathbf{R}(t))c_i(t) - \sum_j \vec{\mu}_{ij}(\mathbf{R}(t)) \cdot \vec{E}(t)c_j(t), \tag{7}$$

where $c_i(t)$ are the expansion coefficients of the electronic wave function in the basis of adiabatic electronic states from which the density-matrix elements can be calculated as $\rho_{ij} = c_i^* c_j$ for i, $j = e$, or g. Notice that the adiabatic state energy is parametrically dependent on the nuclear trajectory $\mathbf{R}(t)$. Equation (7) is solved numerically using the fourth-order Runge-Kutta procedure. The nuclear trajectories $\mathbf{R}(t)$ are obtained by solution of Newton's equations of motion using the Verlet algorithm [21]:

$$M\ddot{\mathbf{R}}(t) = -\sum_i \Theta_i(t)\nabla_R V_i[\mathbf{R}(t)]. \tag{8}$$

In Eq. (8) $\Theta_i(t)$ represents a parameter which has a value of one for the state in which the trajectory is propagated at the given time and zero for all other states and $V_i[\mathbf{R}(t)]$ is the adiabatic potential energy of the electronic state i. The forces acting on the nuclei $\{\nabla_R V_i[\mathbf{R}(t)]\}$ are calculated "on the fly" when they are needed and not from previously parametrized analytic functions. The solution of Eq. (8) provides continuous nuclear trajectories which reside in different electronic states according to the quantum-mechanical occupation

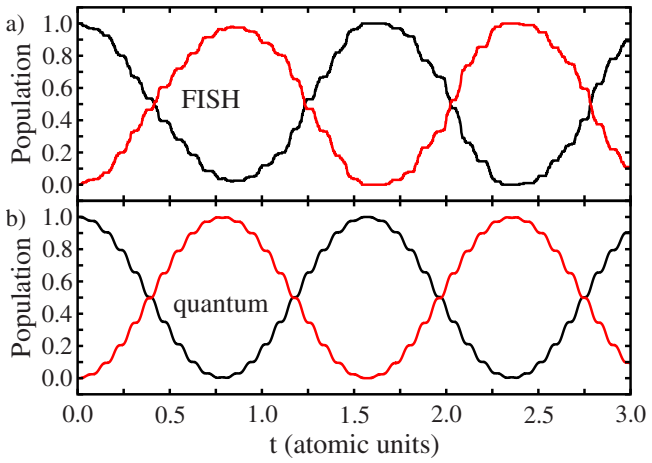

FIG. 1. (Color online) Population dynamics in a two-electronic-state harmonic model system. The ground state is given by $V_g(q)=0.5q^2$ and the excited state by $V_e(q)=0.5q^2+40$. The states are coupled by a resonant electric field with $E(t)=4\ \sin(40\ t)$, the transition dipole moment is $\mu_{ge}=1.0$. (a) Semiclassical populations of the ground (black/dark) and excited (red/light) states. (b) Quantum-mechanical populations of the ground (black/dark) and excited (red/light) states. For quantum dynamics grid based numerical solution of the Schrödinger equation [19] was employed.

probabilities given by ρ_{ee} and ρ_{gg}. Once they are obtained, these trajectories enter the electronic Schrödinger Eq. (7) only as time-dependent continuous parameters. (iii) In order to determine in which electronic state the trajectory is propagated we calculate the hopping probabilities from Eq. (6) and decide if the trajectory is allowed to change the electronic state by using a random number generator. Notice that while the trajectories jump between the electronic states at a given time, all density-matrix elements are propagated continuously over the entire time according to Eq. (7) or Eqs. (1)–(3). Although the individual trajectory is allowed to jump, the total number of trajectories in a given state representing ρ_{ee} or ρ_{gg} is also a continuous function of time. The phase of the electronic wave function is preserved, and our procedure gives rise to the full quantum-mechanical coherent-state population. Therefore our approach is able to mimic laser-induced processes such as coherent Rabi oscillations between the electronic states. In order to illustrate this we present first a comparison of our approach and the full quantum-mechanical treatment of laser-induced dynamics in a two state harmonic oscillator model system. Figure 1 clearly demonstrates the coherent Rabi oscillations which are in perfect agreement with the full quantum-mechanical treatment. Notice that the ability to describe the coherent electronic state dynamics is inherent to our approach and does not depend on the chosen model system. Consequently, the presented FISH procedure represents a general approach for the simulation of laser-induced dynamics in complex molecular systems. In particular, it can be combined with the optimal control theory in order to steer molecular processes. For this purpose the electric field entering Eq. (6) can be iteratively optimized using, e.g., evolutionary algorithms [17,22].

III. RESULTS

In order to demonstrate the accuracy of our FISH method we first present the comparison of full quantum-mechanical and our semiclassical treatments of the optimal control of wave-packet localization in a two-electronic-state model system. The ground electronic state is represented by an asymmetric double-well potential, while for the excited electronic state a Morse potential is used (cf. Fig. 2). In order to selectively transfer the population from the left part of the double well to the right part, we employ the pump-dump [23] optimal control. The laser pulse is analytically parametrized according to $E(t)=\Sigma_i E_i \exp[-\frac{(t-t_i)^2}{2\sigma_i^2}]\sin\{[\omega_i+\gamma_i(t-t_i)](t-t_i)\}$. All pulse parameters are iteratively optimized using a genetic algorithm with binary coding of parameters and the usual selection, crossover, and mutation operations [22]. Notice that the pulse optimization using genetic algorithms is a common technique also used in optimal control experiments [8]. Therefore our optimized pulses are suitable for direct comparison with experiment. We optimize the pulse fully quantum mechanically and apply it subsequently to the system using our semiclassical FISH approach. Alternatively, the pulse can be optimized using the FISH approach first and then applied in a full quantum-mechanical simulation. Both of these approaches yield the same pulse form and optimization efficiency. The quantum mechanically optimized pulse shown in the upper part of Fig. 2(b) consists of two well-separated portions which can be identified as the pump and dump pulses, respectively. This pulse was subsequently used to drive the dynamics of the system by employing our FISH approach. The laser-induced electronic state population dynamics shown in the lower part of Fig. 2(b) for both electronic states demonstrates an excellent agreement between the quantum and FISH simulations. Moreover, the comparison between the snapshots of the wave packets at different times presented in Fig. 2(c) shows that the propagated ensemble of classical trajectories very closely approximates the quantum wave-packet dynamics. Notice that while the coherence between electronic states is exactly included, the FISH method does not account fully for nuclear coherence, and therefore it cannot describe nuclear wave-packet interference, which is not needed for pump-dump control. Therefore, our approach describes accurately the laser-driven ultrafast dynamics and can be used to simulate and control the dynamics in complex systems, where full quantum dynamical simulations are not feasible.

The applicability of our method to the control of laser-driven dynamics in complex molecular systems will be illustrated on the example of the optimal pump-dump photoisomerization of the prototype Schiff base molecular switch N-methylethaniminium (N-MEI) with the chemical composition $[CH_3NH{=}CHCH_3]^+$. Such switchable molecules are used by nature as photoreceptors in the vision process and can be also employed as building blocks for molecular electronic devices. Thus, the control and the mechanism of selective photoswitching by tailored laser fields represents a challenge. The N-MEI has two isomers in the ground electronic state. Its global minimum structure is the trans isomer while the energy of the cis isomer is 0.13 eV higher. In order

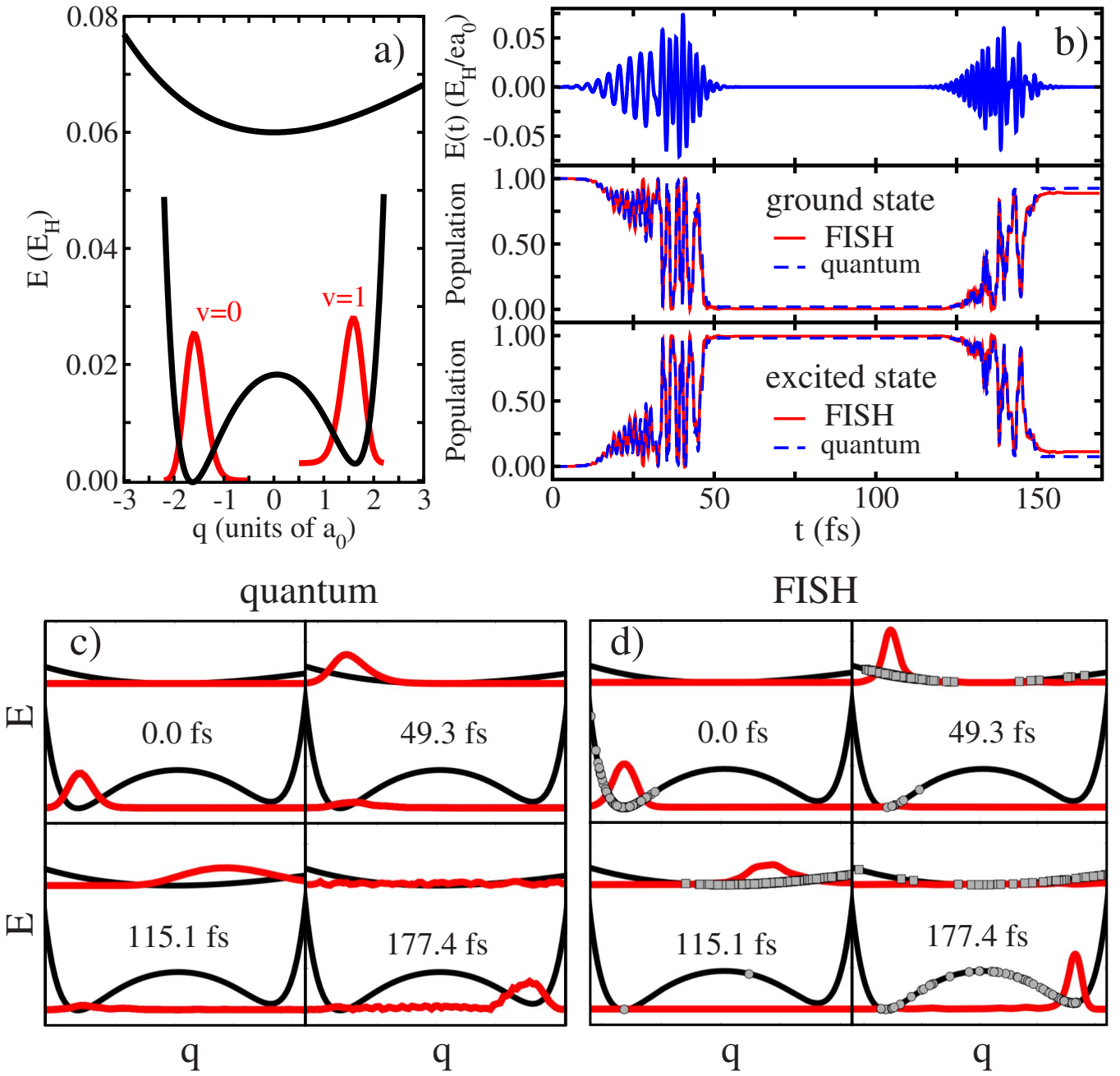

FIG. 2. (Color online) (a) Schematic of the two-electronic-state model system. The double-well potential for the ground state is given by $V_g(q)=0.025789\{\exp[-1.52(q+1.63)]-1\}^2+0.022513\{\exp[-1.56(1.63-q)]-1\}^2+0.022513$ and the Morse potential for the excited state by $V_e(q)=0.09[\exp(-0.12q)-1]^2+0.06$. The two lowest vibrational eigenfunctions of the ground-state potential are shown (red/light curves). (b) (Upper panel): optimized laser field; (middle panel): quantum (blue, dashed line) and FISH (red, full line) populations of the ground electronic state; (lower panel): quantum (blue, dashed line) and FISH (red, full line) populations of the excited electronic state. For quantum dynamics grid based numerical solution of the Schrödinger equation [19] was employed. (c) Snapshots of the quantum wave-packet dynamics, and (d) snapshots of the FISH propagated ensemble of 400 trajectories represented by circles for the ground state and squares for the excited state. Continuous distributions are obtained by convoluting each trajectory with a Gaussian function and are represented by red (light) curves for the sake of comparison with (c).

to control the trans-cis isomerization we employ the semiempirical AM1 configuration interaction (CI) method [24] for the description of the electronic states and for propagation of trajectories without precalculation of potential-energy surfaces accounting for all 30 degrees of freedom. Inclusion of all degrees of freedom in molecular dynamics is of conceptual importance even in the cases that few degrees of freedom might appear to dominate the dynamics. This is warranted by MD on the fly. The AM1 CI method reproduces reasonably accurately both the spectroscopic properties as well as the shape of the potential-energy surfaces of small Schiff base molecules [25]. In order to selectively populate

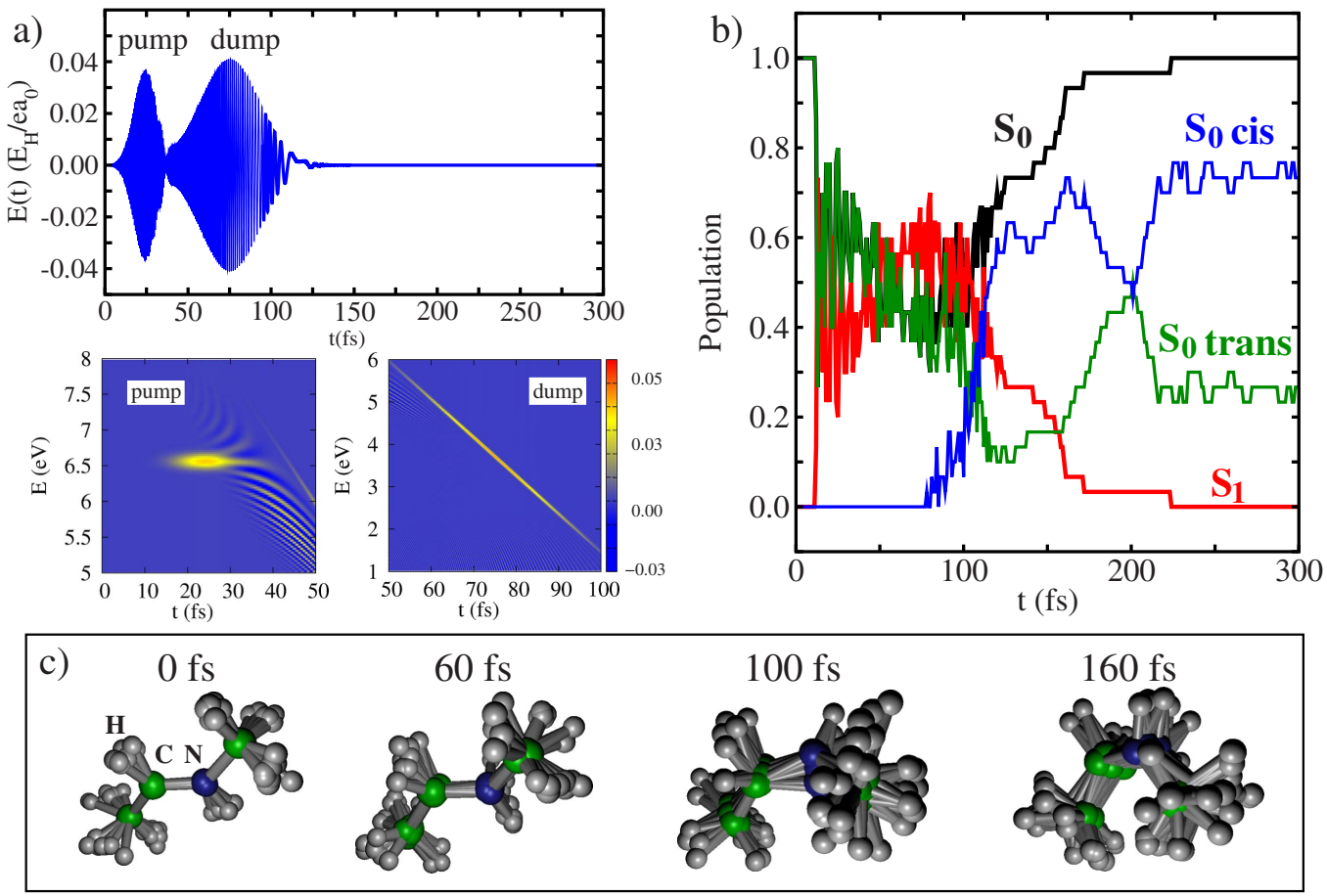

FIG. 3. (Color online) (a) (Upper): optimal pump-dump pulse driving the trans-cis isomerization of N-MEI, (lower): Wigner-Ville transform of the optimal pump (left) and dump (right) pulse showing the temporal distribution of the pulse energies. The intensity is represented by a color bar. The Wigner-Ville transform is defined as $W(t,\omega)=2\,\mathrm{Re}\int_0^\infty d\tau\; e^{-i\omega\tau}E^*(t+\tau/2)E(t-\tau/2)$. (b) Time-dependent populations of the S_0 (black) and S_1 (red) electronic states. For the ground state, also the populations of the trans (green) and the cis (blue) isomers are shown. The Rabi oscillations are present during first 100 fs. (c) Snapshots of the laser-induced dynamics (green, blue, and gray circles label C, N and H atoms, respectively).

the cis isomer, we have optimized the analytically parametrized laser field with a genetic algorithm using the same parametric pulse form as in the model example above. This was achieved by minimizing the target functional $J[t_f]=[180-|\phi(t_f)|]+500\;E_{kin}(t_f)$ accounting both for a maximal torsion angle ϕ and a minimal kinetic energy of the molecule, preventing thermal back isomerization. The ensemble for the pulse optimization consisted of 30 trajectories sampled from a 10 K canonical Wigner distribution. The convergence has been tested by applying the optimal pulse to an ensemble of 100 trajectories. The optimal pulse shown in the upper part of Fig. 3(a) consists of two parts which are nearly overlapping. The maximum intensity of the optimal pulse is 1.7×10^{14} W cm^{-2} which is in the regime of strong but not ultrastrong fields. The temporal structure of the optimal pulse obtained by the Wigner-Ville transformation [cf. bottom part of Fig. 3(a)] shows that the pump subpulse has constant energy centered around 6.6 eV while the dump pulse is linearly down chirped. The energy of the dump pulse varies from 6 eV to less than 2 eV in the time interval between 50 and 100 fs [cf. Fig. 3(a)]. Such large bandwidth has been recently realized by white light continuum pulse shaping [26]. The laser-induced population dynamics presented in Fig. 3(b) shows that the pump pulse depopulates the ground state after ~20 fs. During the subsequent 100 fs the populations of the ground and excited states exhibit Rabi oscillations around the average value of 50%. Within this period, the dump pulse successively depopulates the excited electronic state before the energy gap closes and the conical intersection is reached, steering the dynamics toward the cis isomer. Since during the excited-state dynamics the energy gap between the excited and the ground electronic state becomes smaller as the system performs the rotation around the C=N bond [cf. Fig. 3(c)] the energy of the dump pulse decreases with time (down-chirp) in order to satisfy the resonance condition. The selectivity of the isomerization process is reflected in the time-dependent population of the cis and trans isomers [cf. Fig. 3(b)] giving rise to the final occupation of the cis isomer of ~75%. The occupation of the cis isomer is not 100% due to competing pathways through the conical intersection which start to dominate after the pulse terminates. This is the reason why the population of the cis isomer changes after the laser pulse has been switched off. Notice that excitation with an unshaped pump pulse and sub-

sequent field-free isomerization through the conical intersection between the first excited singlet state and the ground state leads to the cis isomer with the yield of only ~30%. The snapshots of the laser-controlled dynamics shown in Fig. 3(c) illustrate the mechanism of the control involving the rotation around the C=N bond and clearly demonstrate that the cis isomer is optimally reached within 160 fs, suppressing the pathway through the conical intersection. Thus, the optimal pump-dump control can be used to efficiently drive the selective photoisomerization of molecular switches.

IV. CONCLUSIONS

In summary, we have presented the semiclassical FISH method for the simulation and control of ultrafast laser-driven coupled electron-nuclear dynamics involving several electronically excited states in complex molecular systems. This approach combines classical MD simulations with the field-induced surface hopping for the electronic state population dynamics. It can be used to simulate spectroscopic observables as well as to control the dynamics employing shaped laser fields. For the propagation of classical trajectories, the whole spectrum of methods ranging from empirical force fields, semiempirical, to *ab initio* quantum chemical methods can be employed, opening the possibility of broad applications. Therefore, the FISH method offers a powerful tool for the analysis and control of laser-driven excited-state dynamics in complex molecular systems in the gas phase as well as interacting with different environments such as solvent, bioenvironment, surfaces, or metallic nanostructures. In particular, due to the density-matrix formulation of the method, dissipative effects for nuclear and electronic motion can be taken into account. This should in the future give an impetus for the application of the optimal control to manipulate the functionality of complex systems.

ACKNOWLEDGMENTS

This work has been supported by the Deutsche Forschungsgemeinschaft (DFG), SFB 450 project. R.M. acknowledges financial support of the DFG Emmy Noether program (MI-1236/1–1) J.P. thanks the Verband der Chemischen Industrie for financial support.

[1] V. Bonačić-Koutecký and R. Mitrić, Chem. Rev. **105**, 11 (2005).
[2] E. Wigner, Phys. Rev. **40**, 749 (1932).
[3] M. Hillary, R. F. O'Connel, M. O. Scully, and E. P. Wigner, Phys. Rep. **106**, 122 (1984).
[4] A. Donoso and C. C. Martens, Phys. Rev. Lett. **87**, 223202 (2001).
[5] S. A. Rice and M. Zhao, *Optical Control of Molecular Dynamics* (John Wiley & Sons, Inc., New York, 2000).
[6] P. W. Brumer and M. Shapiro, *Principles of the Quantum Control of Molecular Processes* (Wiley-VCH, Berlin, 2003).
[7] D. J. Tannor, *Introduction to Quantum Mechanics: A Time-dependent Perspective* (University Science Books, Sausalito, 2007).
[8] R. S. Judson and H. Rabitz, Phys. Rev. Lett. **68**, 1500 (1992).
[9] A. Assion, T. Baumert, M. Bergt, T. Brixner, B. Kiefer, V. Seyfried, M. Strehle, and G. Gerber, Science **282**, 919 (1998).
[10] C. Daniel, J. Full, L. Gonzalez, C. Lupulescu, J. Manz, A. Merli, S. Vajda, and L. Wöste, Science **299**, 536 (2003).
[11] G. Vogt, G. Krampert, P. Niklaus, P. Nuernberger, and G. Gerber, Phys. Rev. Lett. **94**, 068305 (2005).
[12] B. Schäfer-Bung, R. Mitrić, V. Bonačić-Koutecký, A. Bartelt, C. Lupulescu, A. Lindinger, S. Vajda, S. M. Weber, and L. Wöste, J. Phys. Chem. A **108**, 4175 (2004).
[13] A. P. Peirce, M. A. Dahleh, and H. Rabitz, Phys. Rev. A **37**, 4950 (1988).
[14] R. Kosloff, S. A. Rice, P. Gaspard, S. Tersigni, and D. J. Tannor, Chem. Phys. **139**, 201 (1989).
[15] A. Lindinger, C. Lupulescu, M. Plewicki, F. Vetter, A. Merli, S. M. Weber, and L. Wöste, Phys. Rev. Lett. **93**, 033001 (2004).
[16] B. Schäfer-Bung, V. Bonačić-Koutecký, F. Sauer, S. M. Weber, L. Wöste, and A. Lindinger, J. Chem. Phys. **125**, 214310 (2006).
[17] R. Mitrić and V. Bonačić-Koutecký, Phys. Rev. A **76**, 031405(R) (2007).
[18] R. Mitrić, M. Hartmann, J. Pittner, and V. Bonačić-Koutecký, J. Phys. Chem. A **106**, 10477 (2002).
[19] R. Kosloff, J. Phys. Chem. **92**, 2087 (1988).
[20] J. C. Tully, J. Chem. Phys. **93**, 1061 (1990).
[21] L. Verlet, Phys. Rev. **159**, 98 (1967).
[22] D. E. Goldberg, *Genetic Algorithms in Search, Optimization and Machine Learning* (Addison-Wesley, Reading, MA, 1989).
[23] D. J. Tannor and S. A. Rice, J. Chem. Phys. **83**, 5013 (1985).
[24] M. J. S. Dewar, E. G. Zoebisch, E. F. Healy, and J. J. P. Stewart, J. Am. Chem. Soc. **107**, 3902 (1985).
[25] J. Michl and V. Bonačić-Koutecký, *Electronic Aspects of Organic Photochemistry* (John Wiley & Sons Inc., New York, 1990).
[26] B. E. Schmidt, W. Unrau, A. Mirabal, S. Li, M. Krenz, L. Wöste, and T. Siebert, Opt. Express **16**, 18910 (2008).